

# Zinc isotopes in Late Pleistocene fossil teeth from a Southeast Asian cave setting preserve paleodietary information

Nicolas Bourgon<sup>a,b,c,1</sup>, Klervia Jaouen<sup>a,d</sup>, Anne-Marie Bacon<sup>e</sup>, Klaus Peter Jochum<sup>f</sup>, Elise Dufour<sup>c</sup>, Philippe Durringer<sup>g</sup>, Jean-Luc Ponche<sup>h</sup>, Renaud Joannes-Boyau<sup>i</sup>, Quentin Boesch<sup>g</sup>, Pierre-Olivier Antoine<sup>j</sup>, Manon Hullot<sup>i</sup>, Ulrike Weis<sup>f</sup>, Ellen Schulz-Kornas<sup>a,k,l</sup>, Manuel Trost<sup>a</sup>, Denis Fiorillo<sup>c</sup>, Fabrice Demeter<sup>m,n</sup>, Elise Patole-Edoumba<sup>o</sup>, Laura L. Shackelford<sup>p</sup>, Tyler E. Dunn<sup>q</sup>, Alexandra Zachwieja<sup>p,2</sup>, Somoh Duangthongchit<sup>r</sup>, Thongsasayavongkhamdy<sup>r</sup>, Phonephanh Sichanthongtip<sup>r</sup>, Daovee Sihanam<sup>r</sup>, Viengkeo Souksavady<sup>r</sup>, Jean-Jacques Hublin<sup>a,5</sup>, and Thomas Tütken<sup>b</sup>

<sup>a</sup>Department of Human Evolution, Max Planck Institute for Evolutionary Anthropology, 04103 Leipzig, Germany; <sup>b</sup>Institut für Geowissenschaften, Arbeitsgruppe für Angewandte und Analytische Paläontologie, Johannes Gutenberg-Universität Mainz, 55099 Mainz, Germany; <sup>c</sup>UMR 7209 Archéozoologie, Archéobotanique: Sociétés, Pratiques, Environnements (AASPE), Muséum National d'Histoire Naturelle, CNRS, 75005 Paris, France; <sup>d</sup>Géosciences Environnement Toulouse, UMR 5563, CNRS, Observatoire Midi Pyrénées, 31400 Toulouse, France; <sup>e</sup>CNRS Formation de Recherche en Evolution (FRE) 2029 Biologie, Anthropologie, Biométrie, Epigénétique, Lignées, Université Paris Descartes, Faculté de chirurgie dentaire, 92120 Montrouge, France; <sup>f</sup>Climate Geochemistry Department, Max Planck Institute for Chemistry, 55128 Mainz, Germany; <sup>g</sup>Ecole et Observatoire des Sciences de la Terre (EOST), Institut de Physique du Globe de Strasbourg, UMR 7516 CNRS, Université de Strasbourg, 67084 Strasbourg, France; <sup>h</sup>Laboratoire Image Ville et Environnement, UMR 7362, Institut de Géographie, 67000 Strasbourg, France; <sup>i</sup>Geoarchaeology & Archaeometry Research Group, Southern Cross University, 2480 Lismore, Australia; <sup>j</sup>Institut des Sciences de l'Évolution de Montpellier, Université de Montpellier, CNRS, Institut de Recherche et de Développement (IRD), Ecole Pratique des Hautes Etudes (EPHE), 34090 Montpellier, France; <sup>k</sup>Department of Mammalogy and Palaeoanthropology, Center of Natural History, University of Hamburg, 20146 Hamburg, Germany; <sup>l</sup>Department of Cariology, Endodontology and Periodontology, University of Leipzig, 04109 Leipzig, Germany; <sup>m</sup>Lundbeck Foundation GeoGenetics Centre, University of Copenhagen, 1350 Copenhagen, Denmark; <sup>n</sup>Musée de l'Homme, UMR 7206 Eco-Anthropologie, 75016 Paris, France; <sup>o</sup>Muséum d'Histoire Naturelle, 17000 La Rochelle, France; <sup>p</sup>Department of Anthropology, University of Illinois at Urbana-Champaign, Urbana, IL 61801; <sup>q</sup>Department of Medical Education, School of Medicine, Creighton University, Omaha, NE 68178; <sup>r</sup>Department of Heritage, Ministry of Information, Culture and Tourism, XJ75+CX Vientiane, Lao People's Democratic Republic; and <sup>5</sup>Collège de France, 75005 Paris, France

Edited by Thure E. Cerling, University of Utah, Salt Lake City, UT, and approved January 3, 2020 (received for review July 9, 2019)

**Stable carbon and nitrogen isotope ratios of collagen from bone and dentin have frequently been used for dietary reconstruction, but this method is limited by protein preservation. Isotopes of the trace element zinc (Zn) in bioapatite constitute a promising proxy to infer dietary information from extant and extinct vertebrates. The  $^{66}\text{Zn}/^{64}\text{Zn}$  ratio (expressed as  $\delta^{66}\text{Zn}$  value) shows an enrichment of the heavy isotope in mammals along each trophic step. However, preservation of diet-related  $\delta^{66}\text{Zn}$  values in fossil teeth has not been assessed yet. Here, we analyzed enamel of fossil teeth from the Late Pleistocene (38.4–13.5 ka) mammalian assemblage of the Tam Hay Marklot (THM) cave in northeastern Laos, to reconstruct the food web and assess the preservation of original  $\delta^{66}\text{Zn}$  values. Distinct enamel  $\delta^{66}\text{Zn}$  values of the fossil taxa ( $\delta^{66}\text{Zn}_{\text{carnivore}} < \delta^{66}\text{Zn}_{\text{omnivore}} < \delta^{66}\text{Zn}_{\text{herbivore}}$ ) according to their expected feeding habits were observed, with a trophic carnivore-herbivore spacing of +0.60‰ and omnivores having intermediate values. Zn and trace element concentration profiles similar to those of modern teeth also indicate minimal impact of diagenesis on the enamel. While further work is needed to explore preservation for settings with different taphonomic conditions, the diet-related  $\delta^{66}\text{Zn}$  values in fossil enamel from THM cave suggest an excellent long-term preservation potential, even under tropical conditions that are well known to be adverse for collagen preservation. Zinc isotopes could thus provide a new tool to assess the diet of fossil hominins and associated fauna, as well as trophic relationships in past food webs.**

zinc | stable isotopes | diagenesis | trophic ecology | diet

**S**table isotope analyses in archeology and paleontology have been frequently used to explore the diet of past human populations. Nitrogen stable isotope ( $\delta^{15}\text{N}$ ) analysis of bone or dentin collagen is an established method for the trophic level assessment (1, 2). However, these analyses are confronted with the limitations that arise from the degree of protein preservation (3). Trophic level assessment of ancient mammals and hominins older than ~100 kyr are, due to the lack of collagen preservation, currently out of reach. This timeframe is even shorter (~15 kyr) in arid and wet tropical settings that nonetheless often represent key regions in human evolution, such as Africa (4, 5) and Asia (6,

7). However, beyond the classical collagen-bound nitrogen isotopes, trophic level reconstructions from enamel with different isotope systems have become feasible (8–11) and were recently applied to fossil and archeological specimens (9, 12–15). Using

## Significance

**Dietary habits, especially meat consumption, represent a key aspect in the behavior and evolution of fossil hominin species. Here, we explore zinc (Zn) isotope ratios in tooth enamel of fossil mammals. We show discrimination between different trophic levels and demonstrate that Zn isotopes could prove useful in paleodietary studies of fossil hominin, or other mammalian species, to assess their consumption of animal versus plant resources. We also demonstrate the high preservation potential of pristine diet-related Zn isotope ratios, even under tropical conditions with poor collagen preservation, such as the studied depositional context in Southeast Asia. However, assessing the preservation of original  $\delta^{66}\text{Zn}$  values is required for each fossil site as diagenesis may vary across and even within taphonomic settings.**

Author contributions: N.B., K.J., and T.T. designed research; N.B., K.J., A.-M.B., K.P.J., E.D., P.D., J.-L.P., R.J.-B., Q.B., P.-O.A., M.H., U.W., E.S.-K., M.T., and D.F. performed research; A.-M.B., K.P.J., E.D., F.D., E.P.-E., L.L.S., T.E.D., A.Z., S.D., T.S., P.S., D.S., V.S., and J.-J.H. contributed new reagents/analytic tools; N.B., K.J., A.-M.B., K.P.J., E.D., P.D., J.-L.P., Q.B., P.-O.A., M.H., and T.T. analyzed data; N.B., K.J., A.-M.B., P.D., J.-L.P., R.J.-B., Q.B., and T.T. wrote the paper; and A.-M.B., P.D., J.-L.P., R.J.-B., Q.B., F.D., E.P.-E., L.L.S., T.E.D., A.Z., S.D., T.S., P.S., D.S., and V.S. contributed to excavation and recovery of the materials as part of the Laos Project.

The authors declare no competing interest.

This article is a PNAS Direct Submission.

This open access article is distributed under [Creative Commons Attribution-NonCommercial-NoDerivatives License 4.0 \(CC BY-NC-ND\)](https://creativecommons.org/licenses/by-nc-nd/4.0/).

<sup>1</sup>To whom correspondence may be addressed. Email: nicolas\_bourgon@eva.mpg.de.

<sup>2</sup>Present address: Department of Biomedical Sciences, Medical School, University of Minnesota, Duluth, MN 55812-3031.

This article contains supporting information online at <https://www.pnas.org/lookup/suppl/doi:10.1073/pnas.1911744117/-DCSupplemental>.

First published February 18, 2020.

multi-collector inductively coupled plasma mass spectrometry (MC-ICP-MS) allows for the measurement of “nontraditional” stable isotopes from various elements (calcium, magnesium, zinc [Zn], and strontium [Sr]). Among these, Zn isotope ratios ( $^{66}\text{Zn}/^{64}\text{Zn}$ , expressed as  $\delta^{66}\text{Zn}$  value) constitute a promising dietary indicator (11, 14, 16–18). Indeed, Zn is incorporated as trace element in the enamel bioapatite and, thus, has a better long-term preservation potential compared to collagen-bound nitrogen, showing promise for dietary reconstructions in archeology and paleontology (19). It was not until 2012 that Van Heghe et al. (20) began investigating the causes of the variability of  $\delta^{66}\text{Zn}$  values in a pilot study. Since then, work on mammals from modern food webs, first in Africa (16, 17) and then in the Canadian Arctic (18), have established the relationship between  $\delta^{66}\text{Zn}$  of bioapatite and diet.

As currently understood, two factors influence the variability of  $\delta^{66}\text{Zn}$  values in a food web: the initial Zn isotope composition from the source of intake and biological Zn isotope fractionation occurring within the organism itself. In plants, the initial bioavailable Zn isotope composition is derived from the soil, which is in turn controlled by the nature of the underlying bedrock. Igneous rocks exhibit relatively similar  $\delta^{66}\text{Zn}$  values ( $+0.3 \pm 0.14\%$  [2 $\sigma$ ]) (21, 22). Sedimentary rocks show much more variable  $\delta^{66}\text{Zn}$  values (21–23), with the highest values found in marine carbonates ( $+0.3$  to  $+1.4\%$ ) (24, 25). An initial biological fractionation in plants then occurs between the roots and the soil, which favors the absorption of heavy Zn isotopes relative to the litter layer in which they grow (26–29). An active uptake of heavy Zn isotopes then enhances the intraplant mobility of light Zn isotopes to the most aerial parts of the plants (26–28), leading to a general trend of progressively lower  $\delta^{66}\text{Zn}$  values from root to leaves, i.e., within different parts of a single plant, but also leading to variable  $\delta^{66}\text{Zn}$  values between different plant species (26–28). In animals, the body tissues’  $\delta^{66}\text{Zn}$  values also depend on the Zn isotopic composition of the foods consumed. Different plants and parts of plants consumed will thus induce varying  $\delta^{66}\text{Zn}$  values in herbivores. Similarly, the  $\delta^{66}\text{Zn}$  values of body tissues in carnivores depend on the prey and parts of the prey consumed, with muscles usually exhibiting low  $\delta^{66}\text{Zn}$  values compared to the average Zn isotopic composition of the body (11, 16, 17, 30). Since plants usually have the most elevated  $\delta^{66}\text{Zn}$  values (11, 17) and muscles low values (11, 16, 17, 30), the resulting  $\delta^{66}\text{Zn}$  values of a trophic chain follow an opposite trend as to the classic trophic level tracer  $\delta^{15}\text{N}_{\text{collagen}}$  values, that increase about 3–4‰ per trophic level (2). The higher the trophic level of an animal is, the lower the  $\delta^{66}\text{Zn}$  values of its body tissues are (11, 14, 16–18, 30).

However, while enamel has been shown to be less prone to alteration than bone and dentin (31–36), it is nevertheless not immune from diagenetic processes (34–40). One key predicament to investigating paleoecology through the analysis of trace elements (such as Zn) is thus the absence of diagenetic alteration. Additionally, generalized diagenetic effects on Zn from enamel still remain mostly uncertain, as they seem to vary considerably from site to site (40–42). Therefore, careful investigations of potential postmortem alteration on trace elements in fossil teeth is crucial for each taphonomic setting to separate genuine ecological information from diagenetic alteration such as trace element incorporation, leaching, or replacement (40, 42, 43).

Tam Hay Marklot (THM) cave (filling of the cave, and its associated fauna, dated to 38.4–13.5 ka by U-Th analysis on teeth, *SI Appendix, Supporting Information 1.3, Tables S8–S13, and Figs. S43–S46*), in the northeastern part of Laos, Hua Pan Province, is situated in a subtropical latitudinal setting where preservation of organic material (i.e., collagen) is generally poor (44). This cave offers ideal conditions to rigorously assess the preservation potential of diet-related Zn isotopic composition in fossils, when compared to organic matter-bound dietary proxies such as N isotopes. Indeed, the complex and diverse sedimentary

processes encountered in mainland Southeast Asia often lead to atypical preservation of the vertebrate assemblages, almost always originating from karst breccias (45–47). Subject to a highly variable climate- and water-dependent environment, these karst systems produce fossil assemblages that are often characteristic of long transportation processes through subterranean cave networks, often with multiple reworking episodes (45–47). Furthermore, the surroundings of THM cave offer, at present-day and presumably also in the past, two types of photosynthetic pathways used by local plants,  $\text{C}_3$  and  $\text{C}_4$ , thus allowing an additional and already well-established dietary tracer ( $\delta^{13}\text{C}$ ) of the same specimens to be compared with the  $\delta^{66}\text{Zn}$  results. A detailed description of the regional geology and sedimentary deposits are presented in *SI Appendix, Supporting Information 1.1*.

Here, a multiisotope investigation was carried out on tooth enamel ( $\delta^{66}\text{Zn}$ ,  $^{87}\text{Sr}/^{86}\text{Sr}$ ,  $\delta^{13}\text{C}$ ,  $\delta^{18}\text{O}$ ) and dentin collagen ( $\delta^{15}\text{N}$ ), if still preserved, from the Late Pleistocene (38.4–13.5 ka) fossiliferous assemblage newly recovered in the THM cave in 2015. The preservation of diet-related Zn isotopic composition in fossil enamel was systematically investigated to assess the potential application of Zn isotope analysis for dietary reconstruction in deep time. In order to cover a broad range of distinct trophic levels and dietary habits, tooth enamel from 72 specimens belonging to 22 mammalian taxa was analyzed (*SI Appendix, Table S1*). A variety of small-, medium- and large-sized species were selected, covering a wide range of feeding categories including carnivores, omnivores, and herbivores (where a species’ specific trophic ecology was assigned based on analogous modern-day fauna’s dietary behaviors; *SI Appendix, Table S1*). Enamel from each specimen was sampled for  $\delta^{66}\text{Zn}$ ,  $^{87}\text{Sr}/^{86}\text{Sr}$ ,  $\delta^{13}\text{C}$ , and  $\delta^{18}\text{O}$  isotope analyses ( $>5$  mg per sample for Zn analysis; see *SI Appendix, Supporting Information 3.1*). Because kinetic and equilibrium biological fractionations of  $^{87}\text{Sr}/^{86}\text{Sr}$  are negligible (48–51) and overwritten during normalization for instrumental mass bias (48), radiogenic  $^{87}\text{Sr}/^{86}\text{Sr}$  ratios in animal bones and teeth reflect those of local bioavailable Sr sources (9, 48, 52, 53). Differences in  $^{87}\text{Sr}/^{86}\text{Sr}$  would thus imply provenance from a distinct locality with a different geological bedrock type. The granitic bedrock found at THM locality is likely to exhibit higher  $^{87}\text{Sr}/^{86}\text{Sr}$  associated with concomitant lower  $\delta^{66}\text{Zn}$  values, while the limestone bedrock would show the opposite trend. This could thus explain some of the variability observed in enamel  $\delta^{66}\text{Zn}$  values among the fossil teeth. The carbon isotopic composition ( $\delta^{13}\text{C}$ ) of foods are incorporated into the tissues (i.e., bone and enamel) of the animals that eat them (54, 55). In terrestrial animals, the carbon of food webs is derived from plants that undergo either  $\text{C}_3$  or  $\text{C}_4$  photosynthesis (56), providing a complementary dietary tracer to  $\delta^{66}\text{Zn}$  values. While an array of complex variables are likely to induce variations in the oxygen isotopic composition ( $\delta^{18}\text{O}$ ) of tooth enamel in homeothermic vertebrates (57–59), the present study seeks to explore possible relation between  $\delta^{18}\text{O}$  values and Zn isotopic composition, mostly relative to diet and physiology. A subsample of 23 specimens was also analyzed for dentin collagen  $\delta^{13}\text{C}$  and  $\delta^{15}\text{N}$  values in order to assess the preservation of organic material. When collagen preservation was sufficient (*SI Appendix, Supporting Information 3.5*), the  $\delta^{15}\text{N}$  values ( $n = 4$ ) were compared with  $\delta^{66}\text{Zn}$  of the same specimen since the collagen-bound  $\delta^{15}\text{N}$  values reflect the amount of animal protein in the diet and can thus be used to assess trophic level (2). The impact of postmortem taphonomic alteration processes was assessed in situ with spatially resolved element concentration profiles on six fossil mammalian teeth as well as three modern ones for comparison, with distinct feeding behaviors (carnivorous, omnivorous, and herbivorous), digestive physiologies (foregut, hindgut, and carnivore) and phylogenetic histories (Artiodactyla, Perissodactyla, Carnivora, Rodentia, and Primates). Finally, in order to enhance the interpretative framework of Zn isotopic composition, we

explored the relation between individual factors (diet,  $^{87}\text{Sr}/^{86}\text{Sr}$ ,  $\delta^{13}\text{C}_{\text{apatite}}$ ,  $\delta^{18}\text{O}_{\text{apatite}}$ , zinc concentration, and body mass) with  $\delta^{66}\text{Zn}$  values, by fitting a linear mixed model (LMMs; ref. 60) with a Gaussian error structure and identity link (61). A detailed description of the variation of the different stable isotope systems and the methods used in this study are presented in *SI Appendix, Supporting Informations 2 and 3*.

## Results

Measured  $\delta^{66}\text{Zn}$ ,  $^{87}\text{Sr}/^{86}\text{Sr}$ ,  $\delta^{13}\text{C}$ ,  $\delta^{18}\text{O}$ , and  $\delta^{15}\text{N}$  values for all specimens and reference materials are summarized in *SI Appendix, Supporting Information 4, Tables S3–S5, and Figs. S8–S10*.

The total range of tooth enamel  $\delta^{66}\text{Zn}$  values from THM cave is 1.07‰, ranging from  $-0.04\text{‰}$  to  $+1.03\text{‰}$  (Fig. 1). Herbivores exhibit the highest  $\delta^{66}\text{Zn}$  values ( $\delta^{66}\text{Zn} = +0.68 \pm 0.38\text{‰}$  [ $2\sigma$ ],  $n = 41$ ), carnivores the lowest ( $\delta^{66}\text{Zn} = 0.09 \pm 0.24\text{‰}$  [ $2\sigma$ ],  $n = 9$ ) and the  $\delta^{66}\text{Zn}$  values of omnivores fall in between ( $\delta^{66}\text{Zn} = +0.41 \pm 0.38\text{‰}$  [ $2\sigma$ ],  $n = 22$ ) (Fig. 1 and *SI Appendix, Table S3*). Omnivorous taxa, on average, show the highest variability in the intrataxon ranges of their  $\delta^{66}\text{Zn}$  values (average  $\delta^{66}\text{Zn}$  range =  $0.30 \pm 0.34\text{‰}$  [ $2\sigma$ ]), compared to herbivores (average  $\delta^{66}\text{Zn}$  range =  $0.28 \pm 0.24\text{‰}$  [ $2\sigma$ ]) and carnivores (average  $\delta^{66}\text{Zn}$  range =  $0.15 \pm 0.10\text{‰}$  [ $2\sigma$ ]).

Sixty-nine of 72 specimens were analyzed for  $^{87}\text{Sr}/^{86}\text{Sr}$ . Enamel  $^{87}\text{Sr}/^{86}\text{Sr}$  display a broad range, from 0.7097 to 0.7243 ( $\Delta = 0.0146$ ); however, the majority of specimens clusters between 0.7135 and 0.7173 (52%,  $n = 36$ ; *SI Appendix, Table S3*).

Enamel  $\delta^{13}\text{C}$  values range from  $-16.70\text{‰}$  to  $2.40\text{‰}$  ( $n = 72$ ), covering the full spectrum of values typical for pure subcanopy to open woodland  $\text{C}_3$  and  $\text{C}_4$  plant feeders (Fig. 1*B* and *SI Appendix, Table S3*). Fossil enamel from THM cave indicates that a predominant  $\text{C}_3$  environment existed in the cave surroundings

but with a definite  $\text{C}_4$  grass component (56). The enamel  $\delta^{18}\text{O}$  values range from  $-5.85\text{‰}$  to  $0.2\text{‰}$ .

Collagen preservation of the teeth was poor, as only 4 (*Muntiacus* sp., *Bos* sp., *Sus* sp., and *Rhinoceros sondaicus*) of the 23 dentin samples yielded any collagen and even these fell below the 1% limit ( $\sim 0.46 \pm 0.48\%$  [ $2\sigma$ ]; modern bones =  $\sim 22\%$ ; ref. 3). Nonetheless, collagen extracts have C:N ratios characteristic of well-preserved collagen ( $3.26 \pm 0.08$  [ $2\sigma$ ]) (3) (*SI Appendix, Table S4 and Fig. S9*). The  $\delta^{15}\text{N}_{\text{collagen}}$  values associated with these specimens range from  $+3.15\text{‰}$  to  $+10.56\text{‰}$  and the  $\delta^{13}\text{C}_{\text{collagen}}$  values from  $-24.0\text{‰}$  to  $-9.1\text{‰}$ . The higher  $\delta^{15}\text{N}_{\text{collagen}}$  values are in agreement with associated lower  $\delta^{66}\text{Zn}$  values, for taxa assigned an omnivorous diet (*Sus* sp. and *Muntiacus* sp.), and conversely the lower  $\delta^{15}\text{N}_{\text{collagen}}$  values with higher  $\delta^{66}\text{Zn}$  values, representative of an herbivorous diet (*Bos* sp. and *Rhinoceros sondaicus*). The  $\delta^{13}\text{C}_{\text{collagen}}$  and  $\delta^{13}\text{C}_{\text{apatite}}$  values are also consistent for each specimen (*SI Appendix, Tables S3 and S4*).

Zinc concentration distribution was investigated in 15 cross-sections from 6 fossil mammal teeth and compared to that of 10 cross sections from 3 modern specimens, to assess the impact of postmortem taphonomic processes on the enamel. Additionally, Fe, Mn, Al, Mg, and rare earth elements (REE, calculated as the sum of all measured REE concentrations), which are sensitive to diagenetic alteration, provided complementary tracers to discern the degree of diagenetic alteration of the enamel. Concentrations and distribution profiles of these elements were similar to those of modern teeth and were observed almost systematically across modern and fossil enamel samples, suggesting a lack of any significant diagenetic alteration (uptake or leaching) of trace elements in the latter. Similarly, an absence of relationship between  $\delta^{66}\text{Zn}$  values and average enamel concentration in various other trace elements, with potentially different susceptibilities

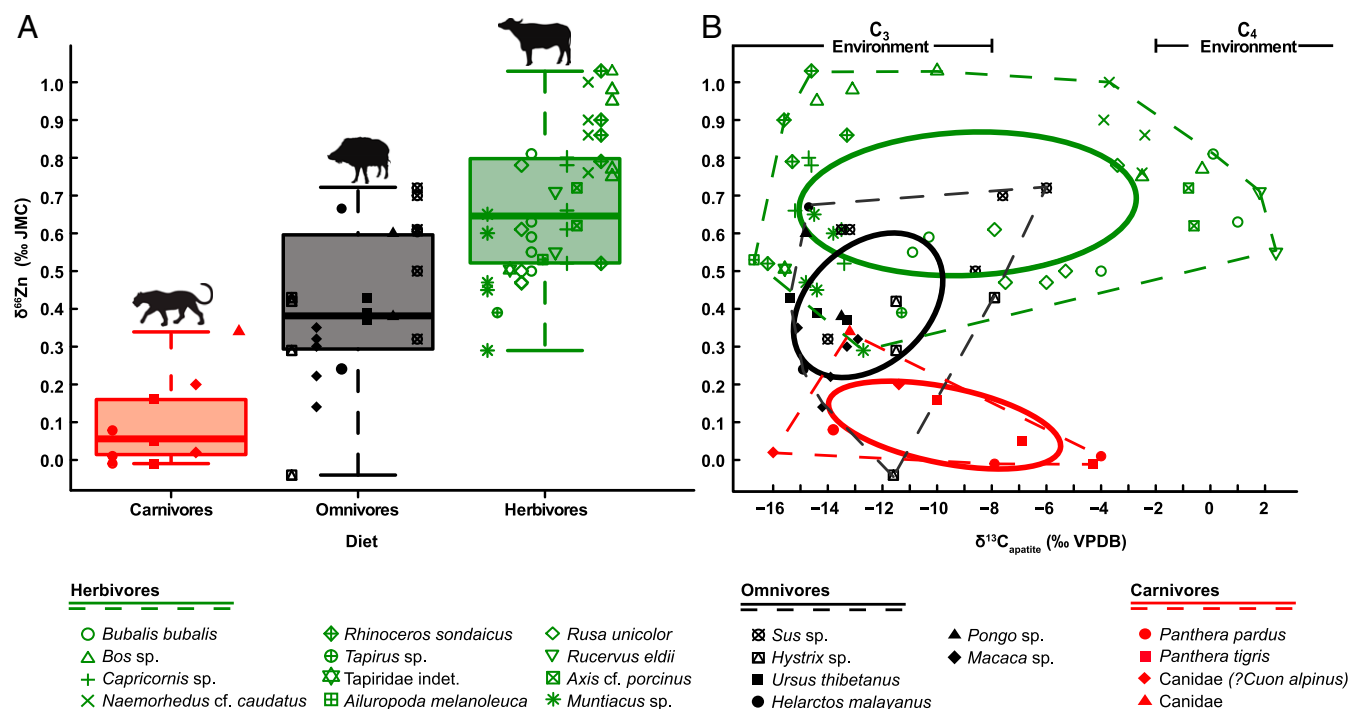


**Fig. 1.** (A) Range of  $\delta^{66}\text{Zn}$  values (relative to the JMC-Lyon Zn isotope standard; ref. 74) in tooth enamel for carnivores (red), omnivores (black), and herbivores (green) of the THM cave assemblage. The boxes within the box and whisker plots represent the 25th–75th percentiles, with the median as a bold horizontal line. (B) Distribution of enamel  $\delta^{66}\text{Zn}$  versus  $\delta^{13}\text{C}_{\text{apatite}}$  values of the THM cave assemblage (*SI Appendix, Table S3*), where “ $\text{C}_3$  environment” and “ $\text{C}_4$  environment” are, respectively, defined by  $\delta^{13}\text{C}_{\text{apatite}} < -8\text{‰}$  and  $> -2\text{‰}$ . Dashed lines represent the full range of variation and full lines represent 40% predictive ellipses (using R statistical software and package “SIBER”; refs. 72 and 75).

for alteration (43), can be observed (*SI Appendix, Figs. S35–S39*). In contrast, the dentin and pulp cavity of the fossil teeth had higher concentrations of these elements indicating diagenetic alteration (Fig. 2). On 15 fossil tooth cross-sections, a total of 23 enamel segments were analyzed. Of these, only one enamel cross-section segment showed Zn concentration distribution that did not follow the characteristic pattern observed for modern enamel ( $n = 10$ ) of higher concentration in the outermost layer that decreases toward a constant level inwards (*SI Appendix, Fig. S30*) (19, 62–64). While the distribution of this one segment may indicate some postmortem alteration, none of the other three enamel cross-section segments analyzed from that same specimen (*Panthera pardus*, 34505) displayed an atypical pattern. The absence of any significant postmortem Zn uptake is nonetheless further corroborated by the absence of a mixing line between Zn concentration and  $\delta^{66}\text{Zn}$  values (*SI Appendix, Fig. S32*). Altogether, a good preservation of the enamel seems to prevail in the fossil specimens, suggesting no alteration of original Zn contents and, hence, preservation of pristine biogenic  $\delta^{66}\text{Zn}$  values. Complete sets of spatial element concentration profiles are provided in *SI Appendix, Figs. S12–S29*.

Overall, the full-null LMM comparison was clearly significant (likelihood ratio test:  $X^2 = 21.29$ ,  $df = 2$ ,  $P < 0.001$ ) and allowed to assess which of the tested predictors were associated with variations in  $\delta^{66}\text{Zn}$  values. The  $\delta^{13}\text{C}$  and  $\delta^{18}\text{O}$  values, as well as the zinc concentration of each sample, appeared to have no significant relation with the variability of the  $\delta^{66}\text{Zn}$  values response ( $\delta^{13}\text{C}_{\text{apatite}}$  values likelihood ratio test:  $X^2 = 0.230$ ,  $df = 1$ ,  $P = 0.632$ ;  $\delta^{18}\text{O}_{\text{apatite}}$  values likelihood ratio test:  $X^2 = 0.135$ ,  $df = 1$ ,  $P = 0.713$ ). Diet had a significant relation with  $\delta^{66}\text{Zn}$  values whereby omnivores and herbivores had clearly elevated values as compared to carnivores (LMM diet  $P < 0.05$ ; *SI Appendix, Table S6*). Finally,  $^{87}\text{Sr}/^{86}\text{Sr}$  and body mass both displayed a significant relation with the variability of the  $\delta^{66}\text{Zn}$  values ( $^{87}\text{Sr}/^{86}\text{Sr}$  likelihood ratio test:  $X^2 = 12.101$ ,  $df = 1$ ,  $P = 0.001$ ; body mass likelihood ratio test:  $X^2 = 9.892$ ,  $df = 1$ ,  $P = 0.002$ ). While (G)LMMs do not allow to get an estimated effect size for individual predictors, the effect size for the entirety of the fixed

effects (“marginal  $R^2$ ”) is 0.63 and the one for the entirety of the fixed and random effects (“conditional  $R^2$ ”) is 0.85 (65).

## Discussion

### Preservation of Diet-Related Zn Isotope Compositions in Fossil Teeth.

The ordering of fossil taxa from THM cave according to their enamel  $\delta^{66}\text{Zn}$  values ( $\delta^{66}\text{Zn}_{\text{carnivores}} < \delta^{66}\text{Zn}_{\text{omnivores}} < \delta^{66}\text{Zn}_{\text{herbivores}}$ ) reflects trophic level differences that are in good agreement with their expected dietary habits (Fig. 1), as well as  $\delta^{66}\text{Zn}$  values observed for modern mammals from similar feeding categories (14, 16–18). This strongly suggests that the enamel of the 38.4–13.5 thousand-year-old fossil teeth from THM cave retained their original, diet-related Zn isotopic composition expected for each feeding category and, hence, was not altered by taphonomic processes. This is further supported by spatial distribution profiles of Zn across the fossil enamel with higher concentrations in the outermost enamel layer decreasing toward a constant level inwards, which is a characteristic pattern for modern teeth (Fig. 2 and *SI Appendix, Figs. S18–S20 and S27–S30*) (19, 62–64). The higher concentration in Zn in the first few tenths of microns of the outermost enamel layer is believed to be a biochemical signal that could be associated with the termination of the enamel maturation (63). While this pattern is systematically observed for all teeth (i.e., both fossil and modern ones), thus supporting the preservation of pristine biogenic Zn concentrations (and thus  $\delta^{66}\text{Zn}$  signatures), it also poses a challenge for distinguishing between original biogenic signature and postmortem diagenetic uptake. However, this layer of higher Zn concentration is systematically only  $< 200\ \mu\text{m}$  thick (Fig. 1 and *SI Appendix, Figs. S12–S29*) (19, 62–64) and, thus, lends further support to the preservation of a biogenic pattern. Furthermore, this outer Zn-rich layer is routinely removed mechanically during the enamel cleaning process for stable isotope analysis.

Due to the tropical setting of THM cave, collagen preservation is limited, as reflected by low collagen extraction success rate (i.e.,  $n = 4$ ) and low collagen yield ( $< 1\%$ ). Nevertheless, the few  $\delta^{15}\text{N}_{\text{collagen}}$  values that were obtained follow the expected trend in  $\delta^{66}\text{Zn}$  values, where relatively high  $\delta^{15}\text{N}_{\text{collagen}}$  values are associated with

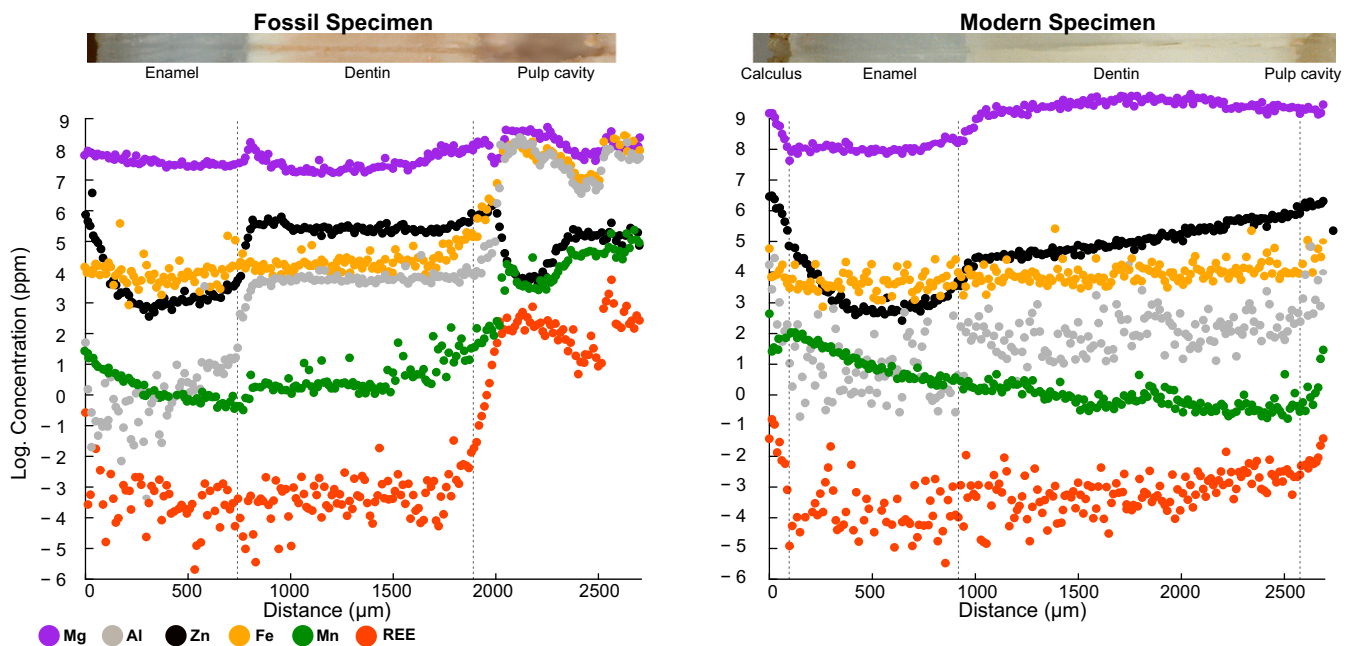


**Fig. 2.** Spatial element concentration profiles of Zn, Fe, Mn, Al, Mg, and REE in caprine teeth for a fossil (*Capricornis* sp., Left) and a modern (*H. jemlahicus*, Right) specimen. The Fe, Mn, Al, and REE (calculated as the sum of all measured REE concentrations) were selected as tracers for diagenetic alteration because of their relative abundance in soil matter, as well as their tendency to be enriched postmortem in fossil bioapatite. Thus, they most likely trace postmortem taphonomic alterations and element uptake from soil pore water. Note that in both photomicrographs the tracks of laser ablation line scans are visible.

relatively low  $\delta^{66}\text{Zn}$  values (18) (*SI Appendix, Fig. S31*). Finally, the low in vivo-like Mn, Fe, Al, Mg, and bulk REE contents, typical for enamel of modern mammal teeth (Fig. 2), demonstrate the lack of any significant diagenetic uptake of trace elements from the soil environment rich in these elements. Although postmortem taphonomic processes can vary significantly from one location to another due to site formations processes, age, environmental conditions, and soil composition (35, 66, 67), multiple lines of evidence presented in this study support the effective preservation of diet-related Zn isotopic composition in enamel of the investigated fossil teeth despite the adverse tropical setting of THM cave. This is encouraging for future applications of Zn isotopes in enamel of fossil teeth for dietary reconstructions.

**Variation in Zn Isotopic Compositions in Tooth Enamel.** The overall mean value and range of  $\delta^{66}\text{Zn}$  values for each diet category, as well as the intraspecific  $\delta^{66}\text{Zn}$  variability of each taxon (*SI Appendix, Supporting Information 4.1*), are in agreement with their dietary habits and display nearly no overlap between carnivores and herbivores. Additionally, the LMM further confirmed that  $\delta^{66}\text{Zn}$  values differ between each of the three dietary categories. Carnivores exhibit the lowest  $\delta^{66}\text{Zn}$  values, in agreement with a strict carnivorous diet, and the smallest range of variation. In contrast, herbivores have significantly higher  $\delta^{66}\text{Zn}$  values than carnivores and many omnivores (Fig. 1). Herbivores also have a broad range of  $\delta^{66}\text{Zn}$  values being consistent with the consumption of a variety of different plants, plant parts, and their specific digestive strategies (foregut and hindgut fermentation). Omnivores display mostly intermediate  $\delta^{66}\text{Zn}$  values but occasionally exhibit values characteristic of carnivorous taxa or strictly herbivorous taxa (Fig. 1). Thus, omnivores exhibit the largest range of  $\delta^{66}\text{Zn}$  values covering all three dietary categories, most likely resulting from a varying proportion of meat (but also of plant and animal matter from vertebrates and invertebrates) in their diet. While not enough data are yet available to draw any definitive conclusions, it is likely that the lower end of their  $\delta^{66}\text{Zn}$  range reflect diets that are mostly composed of animal matter, whereas the upper range would be predominantly, if not entirely, comprised of plants. A single herbivore specimen (*Muntiacus* sp.) falls within the range of carnivores. However, this taxon is known at times to exhibit omnivorous dietary habits, feeding on bird's eggs and small animals (68, 69). Furthermore, its associated high  $\delta^{15}\text{N}$  value attests to a diet that is, at the very least, not strictly limited to plant matter. Finally, both its  $\delta^{66}\text{Zn}$  and  $\delta^{15}\text{N}$  values are similar to that of a *Sus* sp., further supporting an omnivorous diet for this *Muntiacus* specimen.

Overall, the range of  $\delta^{66}\text{Zn}$  values for THM is smaller (1.07‰) than seen in a modern terrestrial food web of the Koobi Fora region of Turkana Basin in Kenya (1.24‰) (17), and the absolute  $\delta^{66}\text{Zn}$  values of the whole food web are also lower. This is likely the result of different faunal assemblages and environments between the two localities: THM cave was situated in a mostly forested setting, whereas Koobi Fora is mainly an open grassland landscape. Because trees are likely to exhibit lower  $\delta^{66}\text{Zn}$  values in their leaves compared to low growing herbaceous vegetation (26–28), this could explain why herbivores, and consequently carnivores, have lower enamel  $\delta^{66}\text{Zn}$  values at THM cave. The Zn isotopic composition of the local geology, seen as having a significant relation with  $\delta^{66}\text{Zn}$  values of THM cave, could also in part explain differences observed between these sites. The trophic spacing observed between mammalian carnivore-herbivore is also larger at THM (+0.60‰) than at Koobi Fora (+0.40‰). This is likely the result of the faunal assemblage from Koobi Fora, as it contains less species and specimens ( $n = 10$  and  $n = 26$ , respectively), carnivores that do not prey on most or any of the herbivores listed, and hyenas' higher  $\delta^{66}\text{Zn}$  values probably caused by bone consumption (17). As opposed to the Koobi Fora region, no clear distinction in

$\delta^{66}\text{Zn}$  values can be drawn between grazers and browsers at THM. However, two groups can be discerned in the  $\delta^{66}\text{Zn}$  values of browsers (established by  $\delta^{13}\text{C}_{\text{apatite}} < -8\text{‰}$  characteristic for  $\text{C}_3$  plant feeders), one with low ( $+0.52 \pm 0.20\text{‰}$  [ $2\sigma$ ],  $n = 14$ ) and the other with high ( $+0.90 \pm 0.20\text{‰}$  [ $2\sigma$ ],  $n = 9$ )  $\delta^{66}\text{Zn}$  values (Fig. 1). In the upper range of the sampled browsers'  $\delta^{66}\text{Zn}$  values (Fig. 1), a mixture of both foregut and hindgut fermenters as well as large and intermediate body-sized taxa are present. Consequently, we conclude that digestive physiology and body mass can be ruled out as factors explaining this variability. Maternal effects linked to breastfeeding or in utero tooth formation were also ruled out as causes to intragroup  $\delta^{66}\text{Zn}$  values variability, as the formation and emergence sequence of the sampled teeth (i.e., only teeth of adult individuals formed postweaning; *SI Appendix, Table S1*) goes against such interpretation. Therefore, the most likely explanation would be diet, most probably linked to the vertical layering of the vegetation in a given habitat. Because of progressively lower  $\delta^{66}\text{Zn}$  values observed within plants from root to leaves, browsing in lower vegetation layers on herbaceous understory plants should lead to higher, grazer-like  $\delta^{66}\text{Zn}$  values, while browsing in upper vegetation layers like the canopy should lead to lower  $\delta^{66}\text{Zn}$  values. This might be the reason for similar  $\delta^{66}\text{Zn}$  values between some browsers (e.g., *Rhinoceros sondaicus* and *Bos* sp.) and grazers (e.g., *Rucervus eldii* and *Axis* cf. *porcinus*, with  $\delta^{13}\text{C}_{\text{apatite}} > -2\text{‰}$  characteristic for  $\text{C}_4$  plant feeders) (Fig. 1).

Finally, the estimates obtained for  $^{87}\text{Sr}/^{86}\text{Sr}$  and body mass from the LMM were in agreement with their respective expectation toward  $\delta^{66}\text{Zn}$  values in a food web (*SI Appendix, Table S6*). Based on the Sr and Zn isotope composition of crustal rocks (21–25, 70), an increase in  $^{87}\text{Sr}/^{86}\text{Sr}$  ratios associated with a decrease in  $\delta^{66}\text{Zn}$  values was expected (*SI Appendix, Table S6*): Granitic bedrock usually exhibits higher  $^{87}\text{Sr}/^{86}\text{Sr}$  associated with concomitant lower  $\delta^{66}\text{Zn}$  values while limestone bedrock show the opposite trend, both present at THM locality. Likewise, a positive relationship between  $\delta^{13}\text{C}$  and body mass due to  $^{13}\text{C}$  enrichment with increasing body mass was reported elsewhere (71) and seems to also apply for  $\delta^{66}\text{Zn}$  values (*SI Appendix, Table S6*). Conversely, no significant relation could be drawn between  $\delta^{13}\text{C}$  and  $\delta^{18}\text{O}$  values and  $\delta^{66}\text{Zn}$  values relative to diet and physiology. The LMM thus allowed us to successfully identify which of the tested predictors showed a significant relation with  $\delta^{66}\text{Zn}$  values, otherwise not always identified as such (*SI Appendix, Fig. S10*). However, their respective impact on  $\delta^{66}\text{Zn}$  values cannot be estimated, although it seems likely that its effect is limited since dietary habits are preserved. Further work (e.g., controlled feeding experiments) will be necessary to ascertain and quantify the impact of these factors on  $\delta^{66}\text{Zn}$  values in a broader and more general context, especially compared to diet.

## Conclusion

In this study, the first Zn isotope dataset of fossil tooth enamel, from a Late Pleistocene Southeast Asian faunal assemblage (~38.4–13.5 ka) from the THM cave in northeastern Laos, Hua Pan Province, is presented. We show multiple lines of evidence that support the lack of significant postmortem diagenetic trace element uptake from the soil environment into the enamel of fossil teeth. Enamel profiles along tooth cross sections do not display any identifiable postmortem alteration of biogenic Zn concentration gradients or diet-related  $\delta^{66}\text{Zn}$  by postmortem processes. The classic trophic-level tracer  $\delta^{15}\text{N}_{\text{collagen}}$  (only obtained for four samples) displayed an expected inverse trophic relation with  $\delta^{66}\text{Zn}$  of the same teeth, further supporting the preservation of original  $\delta^{66}\text{Zn}$  values. The Late Pleistocene mammal teeth from THM thus retained pristine, diet-related  $\delta^{66}\text{Zn}$  values in their tooth enamel that are in good agreement with expected dietary habits of the concerned taxa. For this fossil

food web, a trophic level spacing of  $-0.60\text{‰}$  between herbivores and carnivores was found, while omnivores had intermediate  $\delta^{66}\text{Zn}$  values being  $0.30\text{‰}$  lower or higher to herbivores and carnivores, respectively. Thus, carnivores have the lowest, omnivores intermediate, and herbivores the highest  $\delta^{66}\text{Zn}$  values. Contrary to what was previously observed in an African grassland environment regarding the distinction of browsers and grazers (17), no obvious relation was found between  $\delta^{13}\text{C}$  and  $\delta^{66}\text{Zn}$  values. However, both the local geology and the body mass showed a significant relation with consumer's  $\delta^{66}\text{Zn}$  values, as expected. Further studies from other sites and from controlled feeding experiments will be necessary to ascertain the factors at play and their impact on the variability of  $\delta^{66}\text{Zn}$  values in consumer (hard) tissues. While a systematic, site-specific assessment of the extent of diagenetic alterations of biogenic compositions in fossils is required, the results obtained from THM cave show promise for a high preservation potential of  $\delta^{66}\text{Zn}$  values in fossil enamel. Applying  $\delta^{66}\text{Zn}$  as dietary tracer could thus open new research avenues in paleontology and archeology, providing us with a powerful and much-needed isotopic trophic tracer for prehistoric and geological time periods ( $>100$  kyr) or settings that lack collagen preservation, given pristine  $\delta^{66}\text{Zn}$  values are preserved.

## Methods

**Sample Collection.** The material used in this study consists of a selection of diverse taxa from the THM assemblage, covering a large range of distinct dietary habits. Within each taxon, the same teeth on the dental row (e.g., left p2), or different teeth but with various wear stages (e.g., left and right p2), were selected to ensure they belonged to different individuals. A total of 72 teeth, belonging to 22 distinct species and/or genera, were selected for the present isotopic analysis. One to six specimens per species were used (SI Appendix, Table S1).

**Stable Isotope Analysis.** Zn and Sr isotopic ratios from teeth enamel were measured on a Thermo Scientific Neptune MC-ICP-MS and C and N isotopic ratios from teeth dentin were conducted using a Thermo Finnigan Flash EA coupled to a Delta V isotope ratio mass spectrometer, at the Max Planck Institute for Evolutionary Anthropology in Leipzig, and following the protocols in SI Appendix, Supporting Informations 3.2, 3.3, and 3.5. Stable C and O isotopic composition of every sample were analyzed using a Thermo Delta V Advantage isotopic mass spectrometer coupled to a Thermo Kiel IV Carbonate Device chemical preparator, at the "Service de Spectrométrie de Masse Isotopique du Muséum" in Paris, using the protocol described in SI Appendix, Supporting Information 3.4.

**Spatial Element Concentration Profiles Analytical Technique.** Spatial element concentration profiles were conducted on six fossil teeth (*Capricornis* sp., *Ursus thibetanus*, *P. pardus*, *Sus* sp. *Bubalus bubalis*, and *Macaca* sp.) and three modern teeth (*Bison bison*, *Hemitragus jemlahicus*, and *Pteronura brasiliensis*) of various feeding behaviors (carnivorous, omnivorous, and herbivorous), digestive physiologies (foregut, hindgut, and carnivore) and mammalian order (Artiodactyla, Perissodactyla, Carnivora, Rodentia, and Primates). The measurement routines were performed with a Thermo Scientific Element 2 single collector sector-field ICP-MS coupled with a New Wave UP213 Nd:YAG laser ablation system, at the Max Planck Institute for Chemistry (Mainz), as described in SI Appendix, Supporting Information 3.6.

**Statistical Analysis.** All statistical analyses were performed using the statistical program R (version 3.6.1) (72). To test our hypotheses of predictors associated with variability in  $\delta^{66}\text{Zn}$  values, we fitted a LMM (60) with a Gaussian error structure and identity link (61) using the R-package "lme4" (version 1.1–17) (73). The full method is reported in SI Appendix, Supporting Information 3.7.

A complete description of the material and methods used in this study is presented in SI Appendix, Supporting Information 3. All data discussed in the paper is available to readers in SI Appendix.

**ACKNOWLEDGMENTS.** We thank K. Schilling and B. Brumme (Department of Human Evolution, Max Planck Institute for Evolutionary Anthropology, Leipzig) as well as O. Tombret (UMR 7209 AASPE) for technical support; S. Steinbrenner (Department of Human Evolution, Max Planck Institute for Evolutionary Anthropology, Leipzig) who performed the C and N analysis; R. Mundry (Department of Primatology, Max Planck Institute for Evolutionary Anthropology, Leipzig) for his valuable help and insight with the LMM; R. Barr, C. Zickert, L. Därr, A. Salzer, and L. Schymanski (Multimedia Department, Max Planck Institute for Evolutionary Anthropology, Leipzig) for their help with pictures and figure presentation; Christine Lefèvre, Joséphine Lesur, and Aurélie Verguin of the UMR 7209 (AASPE), Muséum National d'Histoire Naturelle, in Paris, for the agreement and access to the mammal collection; and M. Sponheimer and P. Telouk for their helpful discussions. We would like to acknowledge the support and thank the Max Planck Society and the Deutsche Forschungsgemeinschaft ("PALÄODIET" Project 378496604) for funding this study. T.T. and K.J. received funding by the European Research Council under the European Union's Horizon 2020 research and innovation program Grant Agreements 681450 and 803676, respectively. Funding for the excavation of the Marklot cave in 2015 was provided by the University of Strasbourg (Unistra/EOST UMR 7516) and the Unité Propre de Recherche (UPR) 2147 of CNRS Dynamique de l'évolution humaine, France, and the University of Illinois at Urbana-Champaign. Finally, we would like also to thank V.S. and S. Luangaphay of the Department of National Heritage, Ministry of Information and Culture in Vientiane, Laos, for their authorization to study the Marklot fauna.

1. M. J. Deniro, S. Epstein, Influence of diet on the distribution of nitrogen isotopes in animals. *Geochim. Cosmochim. Acta* **45**, 341–351 (1981).
2. M. J. Schoeninger, M. J. DeNiro, Nitrogen and carbon isotopic composition of bone collagen from marine and terrestrial animals. *Geochim. Cosmochim. Acta* **48**, 625–639 (1984).
3. G. J. van Klinken, Bone collagen quality indicators for palaeodietary and radiocarbon measurements. *J. Archaeol. Sci.* **26**, 687–695 (1999).
4. S. H. Ambrose, Effects of diet, climate and physiology on nitrogen isotope abundances in terrestrial foodwebs. *J. Archaeol. Sci.* **18**, 293–317 (1991).
5. M. van de Loosdrecht *et al.*, Pleistocene North African genomes link Near Eastern and sub-Saharan African human populations. *Science* **360**, 548–552 (2018).
6. C. Clarkson *et al.*, The oldest and longest enduring microlithic sequence in India: 35 000 years of modern human occupation and change at the Jwalapuram Locality 9 rockshelter. *Antiquity* **83**, 326–348 (2009).
7. J. Krigbaum, Reconstructing human subsistence in the West Mouth (Niah Cave, Sarawak) burial series using stable isotopes of carbon. *Asian Perspect.* **44**, 73–89 (2005).
8. N.-C. Chu, G. M. Henderson, N. S. Belshaw, R. E. M. Hedges, Establishing the potential of Ca isotopes as proxy for consumption of dairy products. *Appl. Geochem.* **21**, 1656–1667 (2006).
9. K. J. Knudson *et al.*, Introducing  $\delta^{88/86}\text{Sr}$  analysis in archaeology: A demonstration of the utility of strontium isotope fractionation in paleodietary studies. *J. Archaeol. Sci.* **37**, 2352–2364 (2010).
10. J. E. Martin, D. Vance, V. Balter, Natural variation of magnesium isotopes in mammal bones and teeth from two South African trophic chains. *Geochim. Cosmochim. Acta* **130**, 12–20 (2014).
11. M. Costas-Rodriguez, L. Van Heghe, F. Vanhaecke, Evidence for a possible dietary effect on the isotopic composition of Zn in blood via isotopic analysis of food products by multi-collector ICP-mass spectrometry. *Metallomics* **6**, 139–146 (2014).
12. J. E. Martin, T. Tacail, T. E. Cerling, V. Balter, Calcium isotopes in enamel of modern and Plio-Pleistocene East African mammals. *Earth Planet. Sci. Lett.* **503**, 227–235 (2018).
13. J. E. Martin, D. Vance, V. Balter, Magnesium stable isotope ecology using mammal tooth enamel. *Proc. Natl. Acad. Sci. U.S.A.* **112**, 430–435 (2015).
14. K. Jaouen *et al.*, Tracing intensive fish and meat consumption using Zn isotope ratios: Evidence from a historical Breton population (Rennes, France). *Sci. Rep.* **8**, 5077 (2018).
15. V. Balter *et al.*, Calcium stable isotopes place Devonian conodonts as first level consumers. *Geochim. Perspect. Lett.* **10**, 36–39 (2019).
16. K. Jaouen, M.-L. Pons, V. Balter, Iron, copper and zinc isotopic fractionation up mammal trophic chains. *Earth Planet. Sci. Lett.* **374**, 164–172 (2013).
17. K. Jaouen, M. Beasley, M. Schoeninger, J.-J. Hublin, M. P. Richards, Zinc isotope ratios of bones and teeth as new dietary indicators: Results from a modern food web (Koobi Fora, Kenya). *Sci. Rep.* **6**, 26281 (2016).
18. K. Jaouen, P. Szpak, M. P. Richards, Zinc isotope ratios as indicators of diet and trophic level in Arctic marine mammals. *PLoS One* **11**, e0152299 (2016).
19. C. Dean, A. Le Cabec, K. Spiers, Y. Zhang, J. Garrovetto, Incremental distribution of strontium and zinc in great ape and fossil hominin cementum using synchrotron X-ray fluorescence mapping. *J. R. Soc. Interface* **15**, 20170626 (2018).
20. L. V. Heghe, E. Engström, I. Rodushkin, C. Cloquet, F. Vanhaecke, Isotopic analysis of the metabolically relevant transition metals Cu, Fe and Zn in human blood from vegetarians and omnivores using multi-collector ICP-mass spectrometry. *J. Anal. At. Spectrom.* **27**, 1327–1334 (2012).
21. C. Cloquet, J. Carignan, M. F. Lehmann, F. Vanhaecke, Variation in the isotopic composition of zinc in the natural environment and the use of zinc isotopes in biogeosciences: A review. *Anal. Bioanal. Chem.* **390**, 451–463 (2008).

22. F. Moynier, D. Vance, T. Fujii, P. Savage, The isotope geochemistry of zinc and copper. *Rev. Mineral. Geochem.* **82**, 543–600 (2017).
23. C. N. Maréchal, E. Nicolas, C. Douchet, F. Albarède, Abundance of zinc isotopes as a marine biogeochemical tracer. *Geochim. Geophys. Geosyst.* **1**, 1015 (2000).
24. J.-M. Luck, D. Ben Othman, F. Albarède, P. Telouk, "Pb, Zn and Cu isotopic variations and trace elements in rain" in *Geochemistry of the Earth's Surface*, H. Armansson, Ed. (CRC Press, 1999), pp. 199–203.
25. S. Pichat, C. Douchet, F. Albarède, Zinc isotope variations in deep-sea carbonates from the eastern equatorial Pacific over the last 175 ka. *Earth Planet. Sci. Lett.* **210**, 167–178 (2003).
26. D. J. Weiss *et al.*, Isotopic discrimination of zinc in higher plants. *New Phytol.* **165**, 703–710 (2005).
27. J. Viers *et al.*, Evidence of Zn isotopic fractionation in a soil–plant system of a pristine tropical watershed (Nsimi, Cameroon). *Chem. Geol.* **239**, 124–137 (2007).
28. F. Moynier *et al.*, Isotopic fractionation and transport mechanisms of Zn in plants. *Chem. Geol.* **267**, 125–130 (2009).
29. A. M. Aucour, S. Pichat, M. R. Macnair, P. Oger, Fractionation of stable zinc isotopes in the zinc hyperaccumulator *Arabidopsis halleri* and nonaccumulator *Arabidopsis petraea*. *Environ. Sci. Technol.* **45**, 9212–9217 (2011).
30. V. Balter *et al.*, Bodily variability of zinc natural isotope abundances in sheep. *Rapid Commun. Mass Spectrom.* **24**, 605–612 (2010).
31. J. A. Lee-Thorp, N. J. van der Merwe, Aspects of the chemistry of modern and fossil biological apatites. *J. Archaeol. Sci.* **18**, 343–354 (1991).
32. P. Budd, J. Montgomery, B. Barreiro, R. G. Thomas, Differential diagenesis of strontium in archaeological human dental tissues. *Appl. Geochem.* **15**, 687–694 (2000).
33. Y. Dauphin, C. T. Williams, Diagenetic trends of dental tissues. *C. R. Palevol* **3**, 583–590 (2004).
34. V. Michel, Ph. Idefonse, G. Morin, Assessment of archaeological bone and dentine preservation from Lazaret Cave (Middle Pleistocene) in France. *Palaeogeogr. Palaeoclimatol. Palaeoecol.* **126**, 109–119 (1996).
35. M. J. Kohn, M. J. Schoeninger, W. W. Barker, Altered states: Effects of diagenesis on fossil tooth chemistry. *Geochim. Cosmochim. Acta* **63**, 2737–2747 (1999).
36. C. N. Trueman, N. Tuross, Trace elements in recent and fossil bone apatite. *Rev. Mineral. Geochem.* **48**, 489–521 (2002).
37. M. Sponheimer, J. A. Lee-Thorp, Oxygen isotopes in enamel carbonate and their ecological significance. *J. Archaeol. Sci.* **26**, 723–728 (1999).
38. M. J. Schoeninger, K. Hallin, H. Reeser, J. W. Valley, J. Fournelle, Isotopic alteration of mammalian tooth enamel. *Int. J. Osteoarchaeol.* **13**, 11–19 (2003).
39. P. Grandjean, F. Albarède, Ion probe measurement of rare earth elements in biogenic phosphates. *Geochim. Cosmochim. Acta* **53**, 3179–3183 (1989).
40. M. Sponheimer, J. A. Lee-Thorp, Enamel diagenesis at South African Australopithec sites: Implications for paleoecological reconstruction with trace elements. *Geochim. Cosmochim. Acta* **70**, 1644–1654 (2006).
41. H. Bocherens, D. B. Brinkman, Y. Dauphin, A. Mariotti, Microstructural and geochemical investigations on Late Cretaceous archosaur teeth from Alberta, Canada. *Can. J. Earth Sci.* **31**, 783–792 (1994).
42. E. A. Hinz, M. J. Kohn, The effect of tissue structure and soil chemistry on trace element uptake in fossils. *Geochim. Cosmochim. Acta* **74**, 3213–3221 (2010).
43. B. Reynard, V. Balter, Trace elements and their isotopes in bones and teeth: Diet, environments, diagenesis, and dating of archeological and paleontological samples. *Palaeogeogr. Palaeoclimatol. Palaeoecol.* **416**, 4–16 (2014).
44. W. J. Pestle, M. Colvard, Bone collagen preservation in the tropics: A case study from ancient Puerto Rico. *J. Archaeol. Sci.* **39**, 2079–2090 (2012).
45. P. Düringer, A.-M. Bacon, T. Sayavongkhamdy, T. K. T. Nguyen, Karst development, breccias history, and mammalian assemblages in Southeast Asia: A brief review. *C. R. Palevol* **11**, 133–157 (2012).
46. A.-M. Bacon *et al.*, Late Pleistocene mammalian assemblages of Southeast Asia: New dating, mortality profiles and evolution of the predator–prey relationships in an environmental context. *Palaeogeogr. Palaeoclimatol. Palaeoecol.* **422**, 101–127 (2015).
47. A.-M. Bacon *et al.*, Testing the savannah corridor hypothesis during MIS2: The Boh Dambang hyena site in southern Cambodia. *Quat. Int.* **464**, 417–439 (2018).
48. R. A. Bentley, Strontium isotopes from the earth to the archaeological skeleton: A review. *J. Archaeol. Method Theory* **13**, 135–187 (2006).
49. T. D. Price *et al.*, Isotopic studies of human skeletal remains from a sixteenth to seventeenth century AD churchyard in Campeche, Mexico: Diet, place of origin, and age. *Curr. Anthropol.* **53**, 396–433 (2012).
50. L. E. Wright, Immigration to Tikal, Guatemala: Evidence from stable strontium and oxygen isotopes. *J. Anthropol. Archaeol.* **31**, 334–352 (2012).
51. D. T. T. Flockhart, T. K. Kyser, D. Chipley, N. G. Miller, D. R. Norris, Experimental evidence shows no fractionation of strontium isotopes ( $^{87}\text{Sr}/^{86}\text{Sr}$ ) among soil, plants, and herbivores: Implications for tracking wildlife and forensic science. *Isotopes Environ. Health Stud.* **51**, 372–381 (2015).
52. W. C. Graustein, " $^{87}\text{Sr}/^{86}\text{Sr}$  ratios measure the sources and flow of strontium in terrestrial ecosystems" in *Stable Isotopes in Ecological Research, Ecological Studies*, P. W. Rundel, J. R. Ehleringer, K. A. Nagy, Eds. (Springer New York, 1989), pp. 491–512.
53. J. Lewis, A. W. G. Pike, C. D. Coath, R. P. Evershed, Strontium concentration, radiogenic ( $^{87}\text{Sr}/^{86}\text{Sr}$ ) and stable ( $\delta^{86}\text{Sr}$ ) strontium isotope systematics in a controlled feeding study. *Sci. Technol. Archaeol. Res.* **3**, 53–65 (2017).
54. M. J. DeNiro, S. Epstein, Influence of diet on the distribution of carbon isotopes in animals. *Geochim. Cosmochim. Acta* **42**, 495–506 (1978).
55. J. A. Lee-Thorp, J. C. Sealy, N. J. van der Merwe, Stable carbon isotope ratio differences between bone collagen and bone apatite, and their relationship to diet. *J. Archaeol. Sci.* **16**, 585–599 (1989).
56. B. N. Smith, S. Epstein, Two categories of  $^{13}\text{C}/^{12}\text{C}$  ratios for higher plants. *Plant Physiol.* **47**, 380–384 (1971).
57. A. Longinelli, Oxygen isotopes in mammal bone phosphate: A new tool for paleohydrological and paleoclimatological research? *Geochim. Cosmochim. Acta* **48**, 385–390 (1984).
58. B. Luz, Y. Kolodny, M. Horowitz, Fractionation of oxygen isotopes between mammalian bone-phosphate and environmental drinking water. *Geochim. Cosmochim. Acta* **48**, 1689–1693 (1984).
59. S. Pederzani, K. Britton, Oxygen isotopes in bioarchaeology: Principles and applications, challenges and opportunities. *Earth Sci. Rev.* **188**, 77–107 (2019).
60. R. H. Baayen, *Analyzing Linguistic Data. A Practical Introduction to Statistics* (Cambridge University Press, 2008).
61. P. McCullagh, J. A. Nelder, *Generalized Linear Models* (CRC Press, ed. 2, 1989).
62. K. M. Lee, J. Appleton, M. Cooke, F. Keenan, K. Sawicka-Kapusta, Use of laser ablation inductively coupled plasma mass spectrometry to provide element versus time profiles in teeth. *Anal. Chim. Acta* **395**, 179–185 (1999).
63. T. Tacail, L. Kovačiková, J. Brůžek, V. Balter, Spatial distribution of trace element Calcium-normalized ratios in primary and permanent human tooth enamel. *Sci. Total Environ.* **603–604**, 308–318 (2017).
64. M. J. Kohn, J. Morris, P. Olin, Trace element concentrations in teeth—A modern Idaho baseline with implications for archeometry, forensics, and palaeontology. *J. Archaeol. Sci.* **40**, 1689–1699 (2013).
65. S. Nakagawa, P. C. D. Johnson, H. Schielzeth, The coefficient of determination  $R^2$  and intra-class correlation coefficient from generalized linear mixed-effects models revisited and expanded. *J. R. Soc. Interface* **14**, 20170213 (2017).
66. Y. Wang, T. E. Cerling, A model of fossil tooth and bone diagenesis: Implications for paleodiet reconstruction from stable isotopes. *Palaeogeogr. Palaeoclimatol. Palaeoecol.* **107**, 281–289 (1994).
67. R. E. M. Hedges, Bone diagenesis: An overview of processes. *Archaeometry* **44**, 319–328 (2002).
68. F. Kurt, "Muntjac deer" in *Grzimek's Encyclopedia of Mammals*, S. P. Parker, Ed. (McGraw-Hill Publishing Company, 1990), pp. 137–139.
69. A. Jackson, Muntiacus muntjak (Indian muntjac). *Animal Diversity Web*. [https://animaldiversity.org/accounts/Muntiacus\\_muntjak/](https://animaldiversity.org/accounts/Muntiacus_muntjak/). Accessed 13 December 2018.
70. C. P. Bataille *et al.*, A bioavailable strontium isotope for Western Europe: A machine learning approach. *PLoS One* **13**, e0197386 (2018).
71. J. V. Tejada-Lara *et al.*, Body mass predicts isotope enrichment in herbivorous mammals. *Proc. Biol. Sci.* **285**, 20181020 (2018).
72. R Core Team, R version 3.6.1 (R Foundation for Statistical Computing, Vienna, Austria, 2018).
73. D. Bates, M. Mächler, B. Bolker, S. Walker, Fitting linear mixed-effects models using lme4. *J. Stat. Softw.* **67**, 1–48 (2015).
74. C. N. Maréchal, P. Télouk, F. Albarède, Precise analysis of copper and zinc isotopic compositions by plasma-source mass spectrometry. *Chem. Geol.* **156**, 251–273 (1999).
75. A. L. Jackson, R. Inger, A. C. Parnell, S. Bearhop, Comparing isotopic niche widths among and within communities: SIBER—Stable Isotope Bayesian Ellipses in R. *J. Anim. Ecol.* **80**, 595–602 (2011).